Journal of Physics and Chemistry of Solids 114 (2018) 58–63

Contents lists available at ScienceDirect

Journal of Physics and Chemistry of Solids

journal homepage: www.elsevier.com/locate/jpcs

The "critical limits for crystallinity" in nanoparticles of the elements: A combined thermodynamic and crystallographic critique

J.L. Pelegrina [a,b,c,*], A. Fernández Guillermet [a,b,c]

[a] Centro Atómico Bariloche, CNEA, R8402AGP San Carlos de Bariloche, Argentina
[b] Instituto Balseiro, CNEA and Universidad Nacional de Cuyo, Argentina
[c] CONICET, Argentina

ARTICLE INFO

Keywords:
Nanoparticles
Amorphous phase
Surface energy
Gibbs energy
Lattice-stability

ABSTRACT

The theme of the present work is the procedure for evaluating the minimum size for the stability of a crystalline particle with respect to the same group of atoms but in the amorphous state. A key goal of the study is the critical analysis of an extensively quoted paper by F.G. Shi [J. Mater. Res. 9 (1994) 1307–1313], who presented a criterion for evaluating a "crystallinity distance" (h) through its relation with the "critical diameter" (d_C) of a particle, i.e., the diameter below which no particles with the crystalline structure are expected to exist at finite temperatures. Key assumptions of Shi's model are a direct proportionality relation between h and d_C, and a prescription for estimating h from crystallographic information. In the present work the accuracy of the Shi model is assessed with particular reference to nanoparticles of the elements. To this end, an alternative way to obtain h, that better realizes Shi's idea of this quantity as "the height of a monolayer of atoms on the bulk crystal surface", is explored. Moreover, a thermodynamic calculation of d_C, which involves a description of the bulk- and the surface contributions to the crystalline/amorphous relative phase stability for nanoparticles, is performed. It is shown that the Shi equation does not account for the key features of the h vs. d_C relation established in the current work. Consequently, it is concluded that the parameter h obtained only from information about the structure of the crystalline phase, does not provide an accurate route to estimate the quantity d_C. In fact, a key result of the current study is that d_C crucially depends on the relation between bulk- and surface contributions to the crystalline/amorphous relative thermodynamic stability.

1. Introduction

There is ample evidence that the sintering and alloying ability, mechanical strength, critical temperatures for phase transitions, catalytic properties and other physicochemical properties of nanoparticles are strongly size-dependent [see, for example [1–6]]. More specifically, it is often hypothesized that the differences between the properties of the nanoparticles and the macroscopic material can be understood in terms of the surface-to-volume ratio, which is a measure of the amount of atoms located at the surface compared to that in the bulk [7,8]. A further, conceptually related issue, is that of the minimum size for a stable crystalline nanoparticle. Since crystallinity is a long-range characteristic of the material, when the fraction of the total number of atoms located at its surface is sufficiently large, a non-crystalline (in the following "an amorphous") phase might become more stable [9]. In a pioneering and extensively quoted paper, Shi [10] suggested that such critical condition would be realized in a spherical nanoparticle of diameter d_C, for which all the atoms are accommodated as if they were located at the surface. This idea was quantitatively expressed by introducing the distance h, which was defined by Shi as "the height of a monolayer of atoms on the bulk crystal surface" [10]. By equating the volume of the spherical nanoparticle of diameter d_C with that of a thin spherical shell of the same diameter and width h, the following relation was established [10].

$$\frac{4}{3}\pi\left(\frac{d_C}{2}\right)^3 = 4\pi\left(\frac{d_C}{2}\right)^2 h \tag{1}$$

The so-determined critical diameter, which is directly related to the distance h through the relation

$$d_C = 6\,h \tag{2}$$

was adopted by Shi to represent a "crystallinity limit", i.e., the size below

* Corresponding author. Av. E. Bustillo 9500, R8402AGP San Carlos de Bariloche, Argentina
E-mail address: jlp201@cab.cnea.gov.ar (J.L. Pelegrina).

https://doi.org/10.1016/j.jpcs.2017.10.042
Received 28 July 2017; Received in revised form 2 October 2017; Accepted 31 October 2017
Available online 2 November 2017

which no particles with the crystalline structure are expected to exist at finite temperatures [10].

In order to apply eq. (2), Shi [10] assumed that h was related to the lattice parameter a of the crystalline material. Specifically, it was postulated without further arguments that $h = a/2$ and $h = a/4$ for the face centered cubic and diamond structures, respectively.

A survey of the standard citation databases indicates that the Shi paper has been extensively quoted (223 times according to Scopus). In particular, the concept of a critical distance has been included in theoretical analyses of the size-dependence of the melting temperature of nanoparticles [11–13], and Shi's values for h have been used to interpret experiments on the solid/liquid transition [14]. Contrasting with the ample use of this approach, it is noteworthy that a critical evaluation of its accuracy has not yet been reported. Such an assessment has been performed in the present work, which has been motivated by the following critical issues.

The first issue concerns the Shi prescription to estimate h. At first glance, one would have expected that the distance between close-packed planes in the face centered cubic structures ($\sqrt{3}\,a/3$) could be a better estimate for "the height of a monolayer of atoms on the bulk crystal surface". Such alternative crystallographic criterion would yield a new set of h values.

The second issue concerns the need for an independent method to determine d_C. Since this critical radius expresses the crystalline/amorphous relative stability, it is natural to expect that a thermodynamic approach would provide additional insight on the d_C values.

Both issues will be addressed in the following work by using information on the elements. Once the new, theoretically based h and d_C values had been determined, a critical discussion of the Shi [10] relation for the crystallinity limit, which is expressed by eq. (2) will be performed.

2. Thermodynamic relations

A "top-down" thermodynamic approach has recently been developed by the current authors to determine the relative stability between the crystalline and the amorphous phases of a nanoparticle as a function of the particle radius [15]. The most general formulation of the approach and its experimental test has been presented elsewhere [15]. In the following, only the relations of relevance for the present work are reviewed.

The Gibbs energy of formation (ΔG^{ϕ}) of a nanoparticle of an element in phase ϕ is expressed as the sum of two contributions:

$$\Delta G^{\phi} = \Delta^0 G^{\phi/st} + \Delta G^{\gamma,\phi} \tag{3}$$

where $\Delta^0 G^{\phi/st}$ is the "lattice-stability" of ϕ relative to the stable structure of the element [16] and $\Delta G^{\gamma,\phi}$ is the surface contribution to Gibbs energy. In the present work the focus is on the crystalline ("cr") and the amorphous ("am") phases, and the reference stable structure will be the crystalline one, i.e., $\Delta^0 G^{cr/st} = 0$. This implies that only the term $\Delta^0 G^{am/st} = \Delta^0 G^{am/cr}$ has to be determined at the temperature of interest (T_0), viz., at $T_0 = 300\ K$.

The second term in eq. (3) can be expressed as [15]:

$$\Delta G^{\gamma,\phi} = \left(\frac{\Sigma}{\Omega}\right) \gamma^{\phi}\, V^{\phi} = \left(\frac{6}{d}\right) \gamma^{\phi}\, V^{\phi} \tag{4}$$

where γ^{ϕ} and V^{ϕ} (ϕ = cr, am) are the surface energy per unit area and molar volume of the material, $\Sigma = \pi\, d^2$ the surface, $\Omega = \pi\, \frac{d^3}{6}$ the volume and d the diameter of the spherical particle. Eq. (4) was applied assuming that both phases have the same shape, viz., spherical. The molar volumes V^{cr} for the elements were taken from Ref. [17]. Lacking a consistent set of values for V^{am}, and taking into account a plausible expansion associated to the transition from the crystalline to the amorphous phase, the approximation $V^{am} = 1.01\ V^{cr}$ was adopted at 300 K.

In this equation the γ^{ϕ} parameter for the amorphous and the crystalline phase is a temperature dependent quantity. Furthermore, the γ^{ϕ} parameters are assumed to depend upon the curvature of the particle. This problem is the subject of an extensive literature, and various alternative equations have been presented to account for the effect of the diameter d of the particle upon γ^{ϕ} [18–20]. In particular, the equation by Tolman [18–20] was adopted

$$\gamma^{\phi}(T) = \left(\frac{d}{d\ +\ 4\,\delta^{\phi}}\right) \gamma^{\phi}_{\infty}(T) \tag{5}$$

In eq. (5), the surface energy parameter $\gamma^{\phi}_{\infty}(T)$ is a solely temperature-dependent quantity which is assessed in the next section, and δ^{ϕ}, which is the so-called Tolman parameter, characterizes the width of the interface [18–20]. In the present work, lacking more specific information, the Tolman parameter of both phases was related to the spacing h between the close-packed planes in the crystalline phase, by introducing the proportionality parameter α, viz.,

$$\delta^{am} = \delta^{cr} = \delta = \alpha\, h (0 \le \alpha \le 1) \tag{6}$$

By combining eqs. (3)–(6), the following expression was obtained for the diameter of the smallest crystalline particle which is stable with respect to the amorphous phase:

$$d_C + 4\,\delta = \frac{6\,\left(V^{cr}\,\gamma^{cr}_{\infty}\ -\ V^{am}\,\gamma^{am}_{\infty}\right)}{\Delta^0 G^{am/cr}(T_0)} \tag{7}$$

The assessment of the thermodynamic information involved in the application of eq. (7) to the elements of the Periodic Table is presented in the following sections.

3. Assessment of thermodynamic properties

The lattice-stability and surface Gibbs energy of the amorphous phases of the elements are poorly known from experiments. On the basis of the satisfactory results obtained in Ref. [15], these properties were modeled by identifying the amorphous with a liquid phase undercooled to very low temperatures, as follows.

3.1. Lattice-stability modeling and estimation methods

The lattice-stability term was modeled by assuming that: i) there will be a glass transition in the undercooled liquid ("ucl") at a temperature T_G usually located between one third and one half of the melting temperature (T_M); ii) below that point the heat capacity of the liquid would be similar to that of the crystalline phase; and, iii) at the glass transition the entropy of the liquid will be more or less approaching the entropy of the crystalline phase. Assuming these widely accepted ideas, and following [21], a qualitative curve for the temperature dependence of the entropy difference between the undercooled liquid and the crystalline phase ($\Delta^0 S^{ucl/cr}$) might be sketched as in Fig. 1a. The curve flattens below T_G and the entropy plateau has a negligible value due to assumption (iii).

The corresponding lattice-stability ($\Delta^0 G^{ucl/cr}$) function is presented in Fig. 1b using a thick black solid line. The current premises imply that the high temperature behavior of the liquid phase ("liq"), denoted as $\Delta^0 G^{liq/cr}$ (blue line in Fig. 1b), has to be extrapolated for temperatures below T_G as an approximately horizontal line to obtain the $\Delta^0 G^{ucl/cr}$ vs. T relation. This expectation is accounted for by the thick black solid line in Fig. 1b, which was drawn by assuming that $\Delta^0 S^{ucl/cr}$ diminishes gradually on cooling from the melting point down to T_G and then goes to zero.

On the basis of the thermodynamic behavior represented in Fig. 1, two alternative evaluations of $\Delta^0 G^{am/cr}(T_0)$ were performed. The first evaluation is based on directly identifying the amorphous phase with the undercooled liquid below T_G, and determining the lattice-stability value to be inserted in eq. (7) as:

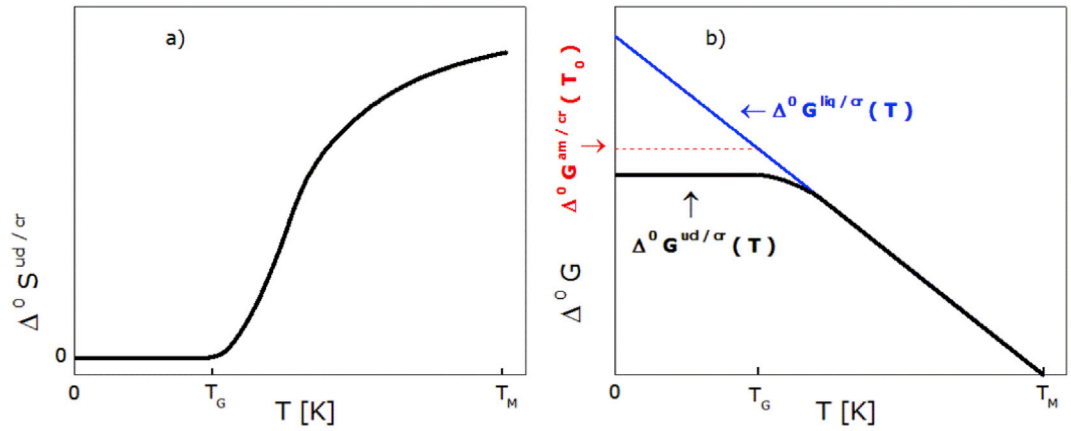

Fig. 1. Qualitative temperature dependence of: a) the entropy difference between the undercooled liquid with a glass transition and the crystalline phase ($\Delta^0 S^{ucl/cr}$) and b) the corresponding lattice-stability ($\Delta^0 G^{ucl/cr}$) function. The determination of the $\Delta^0 G^{am/cr}(T_0)$ value adopted in the present calculations is schematically described by the red thin dashed line. See text for details. (For interpretation of the references to colour in this figure legend, the reader is referred to the web version of this article.)

$$\Delta^0 G^{am/cr}(T_0) = \Delta^0 G^{liq/cr}(T_G) \tag{8}$$

In order to apply eq. (8), it would be necessary to account for the effect of the glass transition upon the $\Delta^0 G^{liq/cr}$ function, i.e., a thermodynamic description of the thick black solid line in Fig. 1b at and below T_G. Unfortunately, such information is not included in the standard databases with lattice-stability values for the elements. In view of this limitation, the $\Delta^0 G^{am/cr}(T_0)$ values were estimated by computing $\Delta^0 G^{liq/cr}$ at T_G and then assuming that the $\Delta^0 G^{am/cr}$ vs. T function continues horizontally down to zero Kelvin, as indicated by the thin red dashed line in Fig. 1b. To this aim, the $\Delta^0 G^{liq/cr}$ vs. T functions recommended by Dinsdale [22] were adopted and the options $T_G = T_M/3$ and $T_G = T_M/2$ were tested.

An alternative evaluation method for $\Delta^0 G^{am/cr}(T_0)$ was based on using the following relation for the enthalpy difference $\Delta^0 H^{am/cr}(T_0)$ between the amorphous and the crystal, suggested on purely empirical grounds by Loeff, Weeber and Miedema [23]:

$$\Delta^0 G^{am/cr}(T_0) = \Delta^0 H^{am/cr}(T_0) \sim 3.5 \left[\frac{J}{K\ mol}\right] T_M \tag{9}$$

3.2. Assessment of lattice-stability values

In the previous paragraph three estimation methods for the lattice-stability of the amorphous phase were presented, viz., the first two using Dinsdale recommended functions at two different glass temperatures and the third one using the approach by Loeff et al. In order to discuss their results, it is useful to compare the relation in eq. (9) with that based on the thin red dashed line in Fig. 1b. The linear behavior of $\Delta^0 G^{liq/cr}$ usually observed in the neighborhood of the equilibrium melting point can be written as

$$\Delta^0 G^{liq/cr}(T) = (T_M - T)\ \Delta^0 S^{liq/cr}(T_M) \tag{10}$$

Then, the first two estimation methods have an upper bound given by

$$\Delta^0 G^{am/cr}(T_0) \sim (T_M - T_G)\ \Delta^0 S^{liq/cr}(T_M) = \left[k\ \Delta^0 S^{liq/cr}(T_M)\right] T_M \tag{11}$$

where $k = 2/3$ or $1/2$, depending on the choice for T_G. The linear extrapolation presented in eq. (10) coincides with the $\Delta^0 G^{liq/cr}$ curve in the whole temperature interval shown in Fig. 1b, which is not the general case. This latter fact is against the relation between $\Delta^0 G^{am/cr}(T_0)$ and the entropy of melting $\Delta^0 S^{liq/cr}(T_M)$ given in eq. (11), which would hold exactly only if the $\Delta^0 G^{liq/cr}$ vs. T function were a straight line in the temperature range $T_G \le T \le T_M$. In spite of this fact, the square bracket

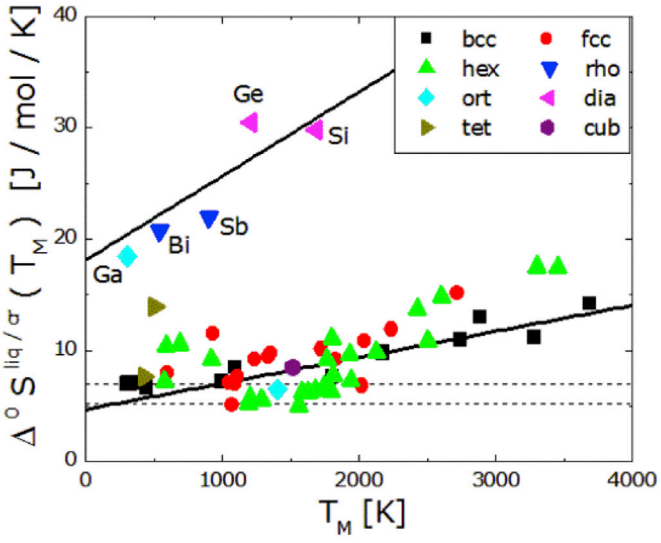

Fig. 2. Entropy difference between the liquid and the crystalline phase evaluated at the melting temperature (T_M) as a function of T_M for 62 elements. The solid lines are only guides to the eye. The horizontal dashed lines indicate the limits of the range of $\Delta^0 S^{liq/cr}(T_M)$ within which eqs. (9) and (11) yield the same results. The upper dashed line corresponds to $k = 1/2$.

in eq. (11) might be adopted as a reasonably first approximation to compare with the coefficient in eq. (9). Since the latter represents an entropy difference, it is natural to compare it with the entropy change involved in eq. (11) viz., $k\ \Delta^0 S^{liq/cr}(T_M)$. Specifically, the suggestion by Loeff et al. [23] is equivalent to inserting in eq. (9) the value $\Delta^0 S^{liq/cr}(T_M) = 3.5/k$, which yields limiting values 5.25 $J/K\ mol$ and 7 $J/K\ mol$ according to the previously stated k values.

These entropy limits are compared in Fig. 2 with the experimental $\Delta^0 S^{liq/cr}(T_M)$ vs. T_M values compiled by Dinsdale [22]. The data points were classified according to the stable crystal structure of the element at room temperature, defining eight classes: body centered cubic (bcc), face centered cubic (fcc), hexagonal (hex), rhombohedral (rho), orthorhombic (ort), diamond (dia), tetragonal (tet) and cubic (cub). The elements treated in the present work might be gathered in two main groups, scattering around the solid lines. These lines are adopted only as guides to the eye. In fact, it has long been suggested [24] that the scatter of the data-points in Fig. 2 might be reduced by treating separately elements with the same structure.

According to Fig. 2 the majority of the data points determine a band

with $\Delta^0 S^{liq/cr}(T_M)$ values lower than about 18 $J\,K^{-1}\,mol^{-1}$ and increasing with T_M. The second group comprises the elements Ga, Bi, Sb, Ge and Si, with larger $\Delta^0 S^{liq/cr}(T_M)$ values increasing also with T_M.

The entropy values compatible with the approach by Loeff et al. [23], indicated by the dashed lines in Fig. 2, fall on the lowest limit of the $\Delta^0 S^{liq/cr}(T_M)$ vs. T_M scatter band. As a consequence, the $\Delta^0 G^{am/cr}(T_0)$ given by eq. (9) would be systematically smaller than those yielded by eq. (8). This expectation is corroborated in Fig. 3, where the lattice-stability values for the 62 elements treated in the present work are plotted as a function of the temperature of melting. The solid lines represent least-squares parabolic fits to the assessed $\Delta^0 G^{liq/cr}(T_M/3)$ (Fig. 3a) and $\Delta^0 G^{liq/cr}(T_M/2)$ (Fig. 3b) results, and the dashed lines represent the $\Delta^0 G^{am/cr}(T_0)$ function given in eq. (9).

This trend in lattice-stability values can be understood in terms of ideas behind the model by Loeff et al. [23]. They emphasized that the lower $\Delta^0 G^{am/cr}(T_0)$ values would account for the possible relaxation of the amorphous towards the crystalline state. In view of these results, the predictions of the method by Loeff et al. [23] were adopted in the present assessment as the lower limits of the probable $\Delta^0 G^{am/cr}(T_0)$ for the elements, and used in Section 4.3 to establish the range of probable d_C by selecting a proper average value to test eq. (2).

3.3. Surface energy contribution

The $\gamma^{\phi}_{\infty}(T)$ values for the crystalline and the amorphous phase at $T = 300\,K$ to be inserted in eq. (7) were assessed from the results in the literature using the approximation $\gamma^{am}_{\infty}(300\,K) \sim \gamma^{liq}_{\infty}(300\,K)$, where $\gamma^{liq}_{\infty}(300\,K)$ is the extrapolated surface tension of the liquid. The assessment procedure was as follows.

First, recommended values of $\gamma^{cr}_{\infty}(0\,K)$ for the solid elements and for $\gamma^{liq}_{\infty}(T_M)$ were taken from Refs. [17] and [25]. The consistency of the information was checked by calculating the $\gamma^{cr}_{\infty}(T_M)$ from the $\gamma^{cr}_{\infty}(0\,K)$ values and the corresponding slopes $(\partial\gamma^{cr}_{\infty}/\partial T)$ recommended in Ref. [26]. Then the ratios $\gamma^{cr}_{\infty}(T_M)/\gamma^{liq}_{\infty}(T_M)$ of 62 elements were evaluated and are presented in Fig. 4 as a function of T_M. The resulting ratios could be represented by the mean value 1.2 ± 0.1 (indicated by the horizontal lines), which compares very well with probable ratios between 1.15 and 1.20 according to Chatain [27]. Next, the $\gamma^{cr}_{\infty}(300\,K)$ were calculated by linearly extrapolating the $\gamma^{cr}_{\infty}(0\,K)$ values to room temperature, and the $\gamma^{liq}_{\infty}(300\,K)$ were obtained by assuming that the ratios $\gamma^{cr}_{\infty}(T_M)/\gamma^{liq}_{\infty}(T_M)$ also hold at room temperature, i.e. $\gamma^{cr}_{\infty}(T_M)/\gamma^{liq}_{\infty}(T_M) = \gamma^{cr}_{\infty}(300\,K)/\gamma^{liq}_{\infty}(300\,K)$. The resulting values are listed in Table 1.

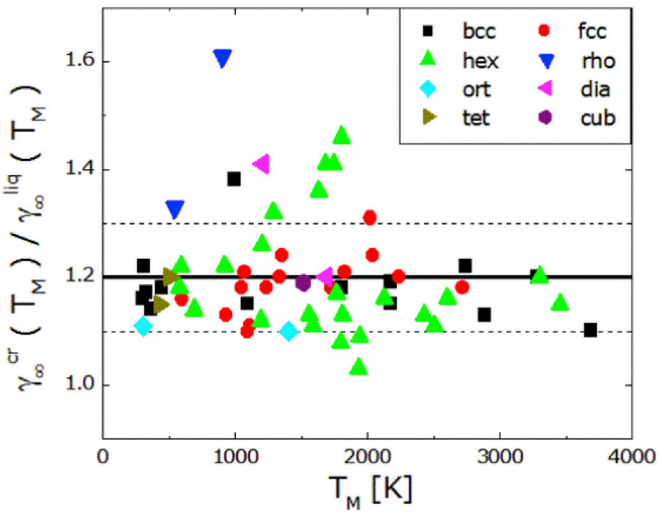

Fig. 4. Ratio of the surface energy term of the crystal to the surface tension of the liquid for 62 elements evaluated at T_M as a function of T_M.

4. Results and discussion

4.1. Predicted $d_C + 4\delta$ values

Values of the quantity $d_C + 4\,\delta$ were obtained by inserting in eq. (7) the surface energy values and the lattice-stability results obtained in the previous section using eq. (8) with $T_G = T_M/3$ and $T_G = T_M/2$ as well as using eq. (9). It is found that the difference between the values based on both choices for T_G is relatively small, whereas larger deviations appear when comparing with those obtained from eq. (9). In particular, the largest differences between the values based on $T_G = T_M/3$ and the estimate based on eq. (9) are found for the following elements: Sb (6.35 nm), Bi (6.25 nm), Ge (4.43 nm), Sn (3.77 nm), Er (3.18 nm), Ga (3.15 nm), Ho (2.70 nm), Cd (2.37 nm), Ba (2.18 nm), Dy (2.02 nm), Si (1.98 nm), Pt (1.68 nm), Nb (1.58 nm) and In (1.55 nm). For the remaining elements the differences are less than 1.5 nm. As a first approximation, each element was assigned a $d_C + 4\,\delta$ value corresponding to the average of those based on eq. (8) with $T_G = T_M/3$ and eq. (9).

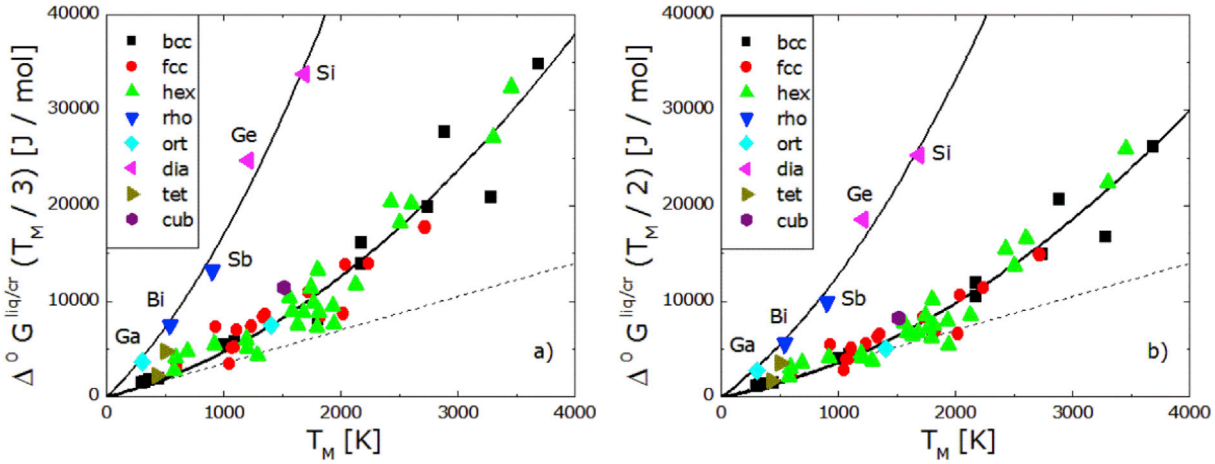

Fig. 3. The lattice-stability of the amorphous relative to the crystalline stable phase, evaluated in the current work as: a) $\Delta^0 G^{liq/cr}(T_M/3)$ and b) $\Delta^0 G^{liq/cr}(T_M/2)$ as functions of the melting temperature for 62 elements, compared with the value obtained on the basis of eq. (9) (dashed lines). The solid lines represent least-squares parabolic fits to the assessed $\Delta^0 G^{liq/cr}(T_M/3)$ and $\Delta^0 G^{liq/cr}(T_M/2)$ results.

Table 1
The assessed values of the surface energy of the solid and surface tension of the liquid at $T_0 = 300\ K$; the quantity $d_C + 4\delta$ given by eq. (7) and the distance h between closest-packed planes in the stable structure of the pure elements.

Element	$\gamma_\infty^{cr}(300\ K)$ [J m^{-2}]	$\gamma_\infty^{liq}(300\ K)$ [J m^{-2}]	$d_C + 4\,\delta$ [nm]	h [nm]
Ag	1.205	1.022	1.96	0.2358
Al	1.146	1.015	1.60	0.2338
Au	1.508	1.261	2.38	0.2354
Ba	0.352	0.254	5.14	0.3555
Be	1.837	1.624	0.81	0.1792
Bi	0.523	0.395	5.25	0.3268
Ca	0.466	0.420	1.31	0.3226
Cd	0.738	0.604	3.63	0.2809
Ce	1.000	0.826	4.77	0.2979
Co	2.490	2.123	1.80	0.2034
Cr	2.349	1.968	1.63	0.2058
Cs	0.080	0.069	3.62	0.4342
Cu	1.793	1.447	2.30	0.2087
Dy	1.100	0.780	5.02	0.2828
Er	1.130	0.776	4.49	0.2794
Eu	0.410	0.357	1.85	0.3239
Fe	2.493	2.116	2.14	0.2027
Ga	0.794	0.718	2.86	0.2260
Gd	1.070	1.966	1.63	0.2891
Ge	0.991	0.705	3.13	0.2000
Hf	2.110	1.896	1.32	0.2525
Ho	1.110	0.788	4.43	0.2808
In	0.654	0.570	4.17	0.2718
Ir	3.052	2.577	1.85	0.2216
K	0.132	0.113	3.67	0.3767
La	0.876	0.784	2.31	0.3036
Li	0.488	0.413	3.25	0.2482
Lu	1.185	1.154	0.26	0.2776
Mg	0.754	0.621	2.62	0.2606
Mn	1.540	1.295	1.41	0.2101
Mo	2.908	2.571	1.12	0.2225
Na	0.230	0.201	2.57	0.3034
Nb	2.658	2.182	2.28	0.2333
Nd	1.040	0.790	6.74	0.2950
Ni	2.390	2.019	1.78	0.2035
Os	3.455	2.875	1.71	0.2158
Pb	0.577	0.496	3.30	0.2858
Pd	2.052	1.703	2.43	0.2246
Pr	1.040	0.827	5.55	0.2959
Pt	2.502	2.026	2.64	0.2266
Rb	0.102	0.084	4.68	0.3949
Re	3.602	3.141	1.33	0.2228
Rh	2.702	2.259	2.09	0.2196
Ru	2.999	2.589	1.51	0.2140
Sb	0.650	0.405	5.17	0.3132
Sc	1.170	1.040	1.46	0.2637
Si	1.245	1.039	1.41	0.1920
Sn	0.677	0.563	4.13	0.2062
Sr	0.409	0.348	3.30	0.3513
Ta	3.008	2.498	2.14	0.2334
Tb	1.090	0.801	5.00	0.2847
Tc	3.002	2.651	1.38	0.2193
Th	1.510	1.155	5.22	0.2935
Ti	2.011	1.846	1.30	0.2343
Tl	0.577	0.490	3.64	0.2762
U	1.860	1.685	1.99	0.2478
V	2.552	2.211	1.66	0.2143
W	3.255	2.964	0.79	0.2238
Y	1.073	0.997	1.16	0.2865
Yb	0.460	0.417	1.29	0.3167
Zn	0.966	0.844	1.95	0.2473
Zr	1.917	1.653	2.29	0.2574

4.2. Crystallographic evaluation of **h** distances

The h values corresponding to the idea of "the height of a monolayer of atoms on the bulk crystal surface", were evaluated as the distance between the closest-packed planes, using the lattice parameters and the relations listed in Table 2 for each structure. The results are also presented in Table 1.

Table 2
Crystallographic relations used to calculate the spacing h between the closest-packed planes in each crystal structure, for the elements considered in the present work.

Structure	Elements	h	Closest-packed planes
bcc		$\frac{\sqrt{2}}{2}\,a$	(1 1 0)
fcc		$\frac{\sqrt{3}}{3}\,a$	(1 1 1)
hex		$\frac{1}{2}\,c$	(0 0 2)
rho	Bi, Sb	$\frac{\sqrt{3}}{2}\,\frac{a\,c}{\sqrt{3\,a^2+c^2}}$	(0 1 2) in the hexagonal cell
ort	Ga	$\frac{1}{2}\,a$	(2 0 0)
ort	U	$\frac{1}{2}\,c$	(0 0 2)
dia	Ge, Si	$\frac{1}{2\sqrt{2}}\,a$	(2 2 0)
tet	In	$\frac{a\,c}{\sqrt{a^2+c^2}}$	(1 0 1)
tet	Sn	$\frac{1}{2\sqrt{2}}\,a$	(2 2 0)
cub	Mn	$\frac{1}{3\sqrt{2}}\,a$	(3 3 0)

4.3. Analysis of the **h** vs. $\mathbf{d_C}$ plots

In order to critically test the Shi [10] approach, the $d_C + 4\,\delta$ values obtained in Section 4.1 were combined with two extreme assumptions about the Tolman parameter stated in relation with eq. (6), viz., $\delta = 0$ and $\delta = h$. In this latter case the model predicts that the elements Lu and W should not present the amorphous phase, which cannot in principle be ruled out.

The h vs. d_C plots presented in Fig. 5a and Fig. 5b were constructed with the two previously mentioned Tolman parameters, respectively. The dotted lines in these graphics represent the Shi relation (eq. (2)).

It is evident that the Shi [10] relation does not account for the general trend of the data points in Fig. 5. The reason is that the h parameter varies between about 0.2 nm and 0.4 nm, i.e., a relatively narrow range, compared with that of the critical diameter d_C, which ranges from negative values (for those few elements predicted not to form an amorphous phase) up to about 7 nm. Moreover, it seems possible to represent the data points in Fig. 5 by means of a band whose scatter limits are indicated by the parallel dashed lines. The straight solid lines are described by the equations $(0.212 + 0.018\,d_C)$ (Fig. 5a) and $(0.234 + 0.016\,d_C)$ (Fig. 5b), clearly showing that the variables h and d_C exhibit a very small dependency on each other, if any exists.

It is evident from Fig. 5 that it is not possible to find a simple, direct relation between the assessed h and the predicted d_C. In other words, the critical diameter at which a crystalline particle becomes unstable with respect to the amorphous state cannot be predicted by relying upon a purely crystallographic parameter. In fact, d_C has to be evaluated by thermodynamic calculations of the relative stability of the phases involved. The current work constitutes a first step forward in such research direction.

5. Summary and concluding remarks

The procedure for evaluating the crystallinity limit h presented in the extensively quoted paper by Shi [10] involves an approximate crystallographic argument. In order to test the accuracy of his method, a twofold strategy was applied. First, an alternative evaluation of h that better realizes Shi's idea of the height of a monolayer of atoms on the bulk crystal surface was adopted. Second, a thermodynamic calculation of d_C, which involves a thermodynamic account of the bulk- and surface contributions to the crystalline/amorphous relative phase stability for nanoparticles, was performed.

The relation between the so-established h and d_C was compared with that given by the Shi approach. It is found that his relation does not account for the main trends of the current empirical results. In fact, instead of his proportionality relation between h and d_C, the current results would be better accounted for by a scatter band of about 0.2 nm in width with h values varying weakly with d_C.

The key conceptual result of the current work is that, instead of the h

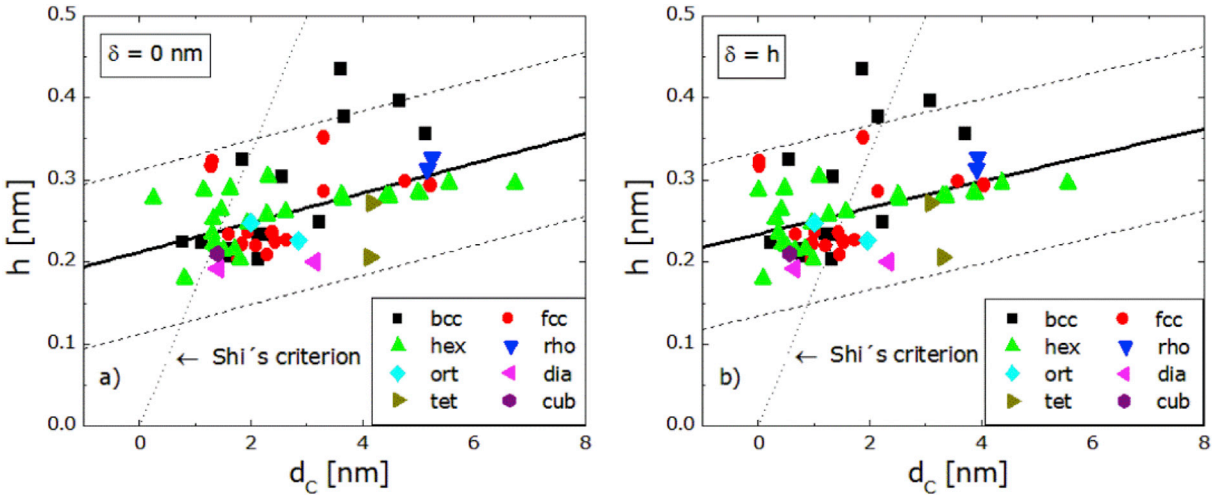

Fig. 5. The distance h between the closest-packed planes as a function of the critical diameter d_C. a) Tolman parameter = 0 nm b) Tolman parameter = h.

parameter, which is based only upon considerations about the structure of the crystalline phase, the crystallinity limit would be more reliably accounted for by the thermodynamically determined quantity d_C. To this aim, additional experimental information on the bulk- and surface contributions to the crystalline/amorphous relative stability for elements at low temperatures is necessary to overcome the limitations of the current database.

Acknowledgements

This work was supported by the ANPCyT, CONICET, CNEA and Universidad Nacional de Cuyo, Argentina. Dr. Julio Andrade Gamboa and Dr. Adriana Condó are gratefully acknowledged for useful suggestions concerning crystallographic aspects.

References

[1] M.A. Asoro, P.J. Ferreira, D. Kovar, In situ transmission electron microscopy and scanning transmission electron microscopy studies of sintering of Ag and Pt nanoparticles, Acta mater. 81 (2014) 173–183.
[2] S. Wang, M. Li, H. Ji, C. Wang, Rapid pressureless low-temperature sintering of Ag nanoparticles for high-power density electronic packaging, Scr. mater. 69 (2013) 789–792.
[3] T.-H. Kao, J.-M. Song, I.-G. Chen, T.-Y. Dong, W.-S. Hwang, Nanosized induced low-temperature alloying in binary and ternary noble alloy systems for micro-interconnect applications, Acta mater. 59 (2011) 1184–1190.
[4] J.D. Nowak, A.R. Beaber, O. Ugurlu, S.L. Girshick, W.W. Gerberich, Small size strength dependence on dislocation nucleation, Scr. mater. 62 (2010) 819–822.
[5] S. Yan, D. Sun, Y. Tan, X. Xing, H. Yu, Z. Wu, Synthesis and formation mechanism of Ag-Ni alloy nanoparticles at room temperature, J. Phys. Chem. Solids 98 (2016) 107–114.
[6] T. Wang, W. Qi, K. Tang, H. Peng, Size dependent structural stability of Mo, Ru, Y and Sc nanoparticles, J. Phys. Chem. Solids 108 (2017) 1–8.
[7] W.H. Qi, M.P. Wang, Size and shape dependent melting temperature of metallic nanoparticles, Mater. Chem. Phys. 88 (2004) 280–284.
[8] S. Bhatt, M. Kumar, Effect of size and shape on melting and superheating of free standing and embedded nanoparticles, J. Phys. Chem. Solids 106 (2017) 112–117.
[9] A. Safaei, M. Attarian Shandiz, Size-dependent thermal stability and the smallest nanocrystal, Phys. E 41 (2009) 359–364.
[10] F.G. Shi, Size dependent thermal vibrations and melting in nanocrystals, J. Mater. Res. 9 (1994) 1307–1313.
[11] Z. Liu, X. Sui, K. Kang, S. Qin, Logarithmic size-dependent melting temperature of nanoparticles, J. Phys. Chem. C 119 (2015) 11929–11933.
[12] M.S. Omar, Models for mean bonding length, melting point and lattice thermal expansion of nanoparticle materials, Mat. Res. Bull. 47 (2012) 3518–3522.
[13] M. Liu, R.Y. Wang, Size-dependent melting behavior of colloidal In, Sn, and Bi nanocrystals, Sci. Rep. 5 (2015) 16353, https://doi.org/10.1038/srep16353.
[14] G. Kellermann, A.F. Craievich, Melting and freezing of spherical bismuth nanoparticles confined in a homogeneous sodium borate glass, Phys. Rev. B 78 (054106) (2008) 1–5.
[15] J.L. Pelegrina, F.C. Gennari, A.M. Condó, A. Fernández Guillermet, Predictive Gibbs-energy approach to crystalline/amorphous relative stability of nanoparticles: size-effect calculations and experimental test, J. Alloys Compd. 689 (2016) 161–168.
[16] L. Kaufman, H. Bernstein, Computer Calculation of Phase Diagrams, Academic Press, New York, 1970.
[17] F.R. de Boer, R. Boom, W.C.M. Mattens, A.R. Miedema, A.K. Niessen, Cohesion in Metals, North-Holland Physics Publishing, Amsterdam, 1988.
[18] G. Kaptay, Nano-Calphad: extension of the Calphad method to systems with nano-phases and complexions, J. Mater. Sci. 47 (2012) 8320–8335.
[19] G. Kaptay, The Gibbs equation versus the Kelvin and the Gibbs-Thomson equations to describe nucleation and equilibrium of nano-materials, J. Nanosci. Nanotech. 12 (2012) 2625–2633.
[20] V.M. Fokin, E.D. Zanotto, Crystal nucleation in silicate glasses: the temperature and size dependence of crystal/liquid surface energy, J. Non-Cryst. Solids 265 (2000) 105–112.
[21] A. Fernández Guillermet, M. Hillert, A thermodynamic analysis of the Calphad approach to phase stability of the transition metals, Calphad 12 (1988) 337–349.
[22] A.T. Dinsdale, SGTE data for pure elements, Calphad 15 (1991) 317–425.
[23] P.I. Loeff, A.W. Weeber, A.R. Miedema, Diagrams of formation enthalpies of amorphous alloys in comparison with the crystalline solid solution, J. Less-Common Met. 140 (1988) 299–305.
[24] N. Saunders, A.P. Miodownik, A.T. Dinsdale, Metastable lattice stabilities for the elements, Calphad 12 (1988) 351–374.
[25] E.A. Brandes, G.B. Brook (Eds.), Smithells Metals Reference Book, seventh ed., Butterworth-Heinemann, Oxford, 1992.
[26] A.R. Miedema, Surface energies of solid metals, Z. Met. 69 (1978) 287–292.
[27] D. Chatain, Anisotropy of wetting, Annu. Rev. Mater. Res. 38 (2008) 45–70.